Chemistry of Iridium Carbonyl Cluster Complexes. Synthesis and X-ray Crystal Structure of [PPh4]2[Ir12(μ-CO)5(CO)19], Containing an Unprecedented Metal Skeleton

Roberto Della Pergola,[1a] Francesco Demartin,[*,1b] Luigi Garlaschelli,[*,1a] Mario Manassero,[1b] Secondo Martinengo,[1a] Norberto Masciocchi,[1b] and Piero Zanello[*,1c]

Dipartimento di Chimica Inorganica, Metallorganica e Analitica, Centro CNR per lo Studio sulla Sintesi e la Struttura dei Composti dei Metalli di Transizione nei Bassi Stati di Ossidazione, and Istituto di Chimica Strutturistica Inorganica, Università degli Studi di Milano, Via G. Venezian 21, 20133 Milano, Italy, and Dipartimento di Chimica, Università degli Studi di Siena, Pian dei Mantellini 44, 53100, Siena, Italy

The new dodecanuclear carbonyl cluster $[Ir_{12}(CO)_{24}]^{2-}$ can be prepared in good yields by thermal treatment of $[Ir_6(CO)_{15}\{Cu(NCMe)\}]^-$ in refluxing tetrahydrofuran: the anion has been characterized as the tetraphenylphosphonium salt by a crystallographic study. $[PPh_4]_2[Ir_{12}(CO)_{24}]$ crystallizes in the triclinic space group $P\bar{1}$ with cell constants $a = 14.614(5)$ Å, $b = 25.435(6)$ Å, $c = 11.977(5)$ Å, $\alpha = 90.30(3)°$, $\beta = 112.94(3)°$, $\gamma = 104.33(2)°$, $V = 3946(5)$ Å^3, and $Z = 2$. Data were collected at room temperature to a maximum $2\theta = 46°$, giving 10 311 unique reflections. The structure was solved by direct methods. The final discrepancy indices were $R = 0.050$ and $R_w = 0.057$ for 5562 independent reflections with $I > 3\sigma(I)$. The metal framework of the anion is a ν_2 (14-atom) trigonal bipyramid, lacking one apical and one equatorial vertex. The Ir–Ir distances are scattered in the range 2.654(1)–2.939(1) Å. Average bond distances for Ir–C$_{terminal}$, Ir–C$_{bridging}$, C–O$_{terminal}$, and C–O$_{bridging}$ are 1.82, 2.05, 1.19, and 1.19 Å, respectively. Electrochemistry shows that the dianion undergoes, in acetonitrile solution, a series of single-stepped two-electron transfers encompassing the sequence 2+/0/2–/4–/6–, mostly leading to transient congeners. Only the dianion/tetraanion redox change appears to be chemically reversible, but its electrochemical features suggest that $[Ir_{12}(CO)_{24}]^{2-}$ must experience severe stereochemical reorganization upon the addition of two electrons.

Introduction

Presently there are three general methods available for the synthesis of large metal carbonyl clusters, e.g. redox condensation, oxidative coupling, and thermal growth, frequently promoted by basic alcoholic solution which causes loss of CO and cluster condensation.[2]

In the case of iridium carbonyl clusters, the $[Ir_6(CO)_{15}]^{2-}$ [3] and $[Ir_9(CO)_{20}]^{3-}$ [4] anions are obtained by reacting $Ir_4(CO)_{12}$ with $[Ir(CO)_4]^-$, these syntheses being examples of the first technique. The reaction between $Ir_4(CO)_{12}$ and alkali metal hydroxides gives rise, according to different experimental conditions, to a series of anionic iridium carbonyl clusters containing up to eight metal atoms, such as $[HIr_4(CO)_{11}]^-$,[3] $[Ir_6(CO)_{15}]^{2-}$,[3] $[Ir_8(CO)_{20}]^{2-}$,[3] and $[Ir_8(CO)_{22}]^{2-}$,[3] most of which have been structurally characterized.[5–7] Under these experimental condi-

tions several other compounds are also formed, since the reactions are not selective, and intractable mixtures of different derivatives are often obtained.

We also reported the preparation, the solid-state structure,[8,9] and the chemical behavior[9] of the dodecanuclear cluster $[Ir_{12}(CO)_{26}]^{2-}$. This compound was obtained by oxidation of $[Ir_6(CO)_{15}]^{2-}$ with the cation $[Cu(NCMe)_4]^+$, and it is the minor component of a mixture containing also $[Ir_6(CO)_{15}\{Cu(NCMe)\}]^-$.[9] The formation of $[Ir_{12}(CO)_{26}]^{2-}$ was the first example of the oxidative coupling reaction.

The preparation of the new $[Ir_{12}(CO)_{24}]^{2-}$, here reported, is a second example of the oxidative coupling method; the preparation of the same large iridium carbonyl clusters from thermally induced reductive condensation was also proved, but was abandoned because of its scarce reproducibility.

The X-ray structure and the extended electrochemistry of $[PPh_4]_2[Ir_{12}(CO)_{24}]$ are also presented.

Experimental Section

All the solvents were purified and dried by conventional methods and stored under nitrogen. All the reactions were carried out under an oxygen-free nitrogen atmosphere using the Schlenk-tube technique.[10] $Ir_4(CO)_{12}$,[11] $[Ir_6(CO)_{15}]^{2-}$,[3] and $[Cu(NCMe)_4]PF_6$[12] were prepared by the published

(1) (a) Dipartimento di Chimica Inorganica, Metallorganica e Analitica e Centro CNR, Università degli Studi di Milano. (b) Istituto di Chimica Strutturistica Inorganica, Università degli Studi di Milano. (c) Università degli Studi di Siena.
(2) (a) Vargas, M. D.; Nicholls, J. N. Adv. Inorg. Chem. Radiochem. 1986, 30, 123. (b) Adams, R. D. In The Chemistry of Metal Cluster Complexes; Shriver, D. F., Kaesz, H. D., Adams, R. D., Eds.; VCH: New York, 1990. (c) Vahrenkamp, H. Adv. Organomet. Chem. 1983, 22, 169. (d) Geoffroy, G. L. In Metal Cluster in Catalysis; Gates, B. C., Guczi, L., Knozinger, H., Eds.; Elsevier: New York, 1986. (e) Roberts, D. A.; Geoffroy, G. L. In Comprehensive Organometallic Chemistry; Wilkinson, G., Stone, F. G. A., Abel, F., Eds.; Pergamon: London, 1982; Chapter 40. (f) Mingos, D. P. M.; Wales, D. J. Introduction to Cluster Chemistry; Prentice-Hall International Edition, Inorganic and Organometallic Chemistry Series; Prentice-Hall: London, 1990.
(3) Angoletta, M.; Malatesta, L.; Caglio, G. J. Organomet. Chem. 1975, 94, 99.
(4) Della Pergola, R.; Demartin, F.; Garlaschelli, L.; Manassero, M.; Martinengo, S.; Masciocchi, N.; Strumolo, D. Inorg. Chem. 1991, 30, 846.
(5) Demartin, F.; Manassero, M.; Sansoni, M.; Garlaschelli, L.; Raimondi, C. C.; Martinengo, S.; Canziani, F. J. Chem. Soc., Chem. Commun. 1981, 528.

(6) Bau, R.; Chiang, M. Y.; Wei, C. Y.; Garlaschelli, L.; Martinengo, S.; Koetzle, T. F. Inorg. Chem. 1984, 23, 4748.
(7) Demartin, F.; Manassero, M.; Sansoni, M.; Garlaschelli, L.; Martinengo, S.; Canziani, F. J. Chem. Soc., Chem. Commun. 1980, 903.
(8) Della Pergola, R.; Demartin, F.; Garlaschelli, L.; Manassero, M.; Martinengo, S.; Sansoni, M. Inorg. Chem. 1987, 26, 3487.
(9) Della Pergola, R.; Garlaschelli, L.; Demartin, F.; Manassero, M.; Masciocchi, N. J. Organomet. Chem. 1992, 436, 241.
(10) Shriver, D. F.; Drezdzon, M. A. In The Manipulation of Air-Sensitive Compounds, 2nd ed.; Wiley: New York, 1986.
(11) Della Pergola, R.; Garlaschelli, L.; Martinengo, S. J. Organomet. Chem. 1987, 331, 271. Della Pergola, R.; Garlaschelli, L.; Martinengo, S. Inorg. Synth. 1990, 28, 245.
(12) Kubas, G. J. Inorg. Synth. 1979, 19, 311.

Table I. Summary of Crystal Data and Intensity Collection Parameters for [PPh₂]₂[Ir₁₂(CO)₂₄] (Estimated Standard Deviations (Esd's) in Parentheses)

chem formula	$C_{72}H_{40}Ir_{12}O_{24}P_2$	γ, deg	104.33(2)
fw	3657.46	V, Å^3	3946(5)
crystal system	triclinic	Z	2
space group	$P\bar{1}$	T, K	298
a, Å	14.614(5)	ρ_{calcd}, g cm^{-3}	3.078
b, Å	25.435(6)	wavelength, Å	0.710 73
c, Å	11.977(5)	linear abs coeff; cm^{-1}	201.8
α, deg	90.30(3)	R^a	0.050
β, deg	112.94(3)	$R_w{}^b$	0.057

^{a} $R = \sum(F_o - k|F_c|)/\sum F_o$. ^{b} $R_w = [\sum w(F_o - k|F_c|)^2/\sum wF_o^2]^{1/2}$.

methods. Infrared (IR) spectra were recorded on a Perkin-Elmer 781 grating spectrophotometer using calcium fluoride cells previously purged with N₂. Materials and apparatus for electrochemistry have been described elsewhere.[13] Direct current voltammograms at a platinum electrode with periodic renewal of the diffusion layer (DCV) have been obtained as previously described.[14] Unless otherwise specified, potential values are calibrated against an aqueous saturated calomel electrode (SCE).

1. Preparation of [PPh₄]₂[Ir₁₂(CO)₂₄] by Thermal Decomposition of [Ir₆(CO)₁₅{Cu(NCMe)}]⁻. A Schlenk tube is filled with a solution of [PPh₄]₂[Ir₆(CO)₁₅] (0.36 g, 0.16 mmol) in tetrahydrofuran (THF) (15 mL) to which solid [Cu(NCMe)₄]PF₆ (0.068 g, 0.18 mmol) is added. The mixture is allowed to react for 30 min at room temperature. Upon dissolution, the color changes readily from brown to red-brown with the formation of [Ir₆(CO)₁₅{Cu(NCMe)}]⁻ and a white precipitate of [PPh₄]-PF₆; the completeness of the reaction is checked by IR, and the white precipitate is filtered off. The resulting red-brown solution is refluxed in an oil bath for about 8 h. To the solution, turned green, a small portion of [Cu(NCMe)₄]PF₆ (0.010 g, 0.025 mmol) is added (to convert back traces of [Ir₆(CO)₁₅]²⁻), and the mixture is heated for 4 h more and then cooled to room temperature. A solution of [PPh₄]Br (0.5 g) in 2-propanol (20 mL) is added; the solvent is partially removed in vacuum until a complete precipitation occurs. The crude brown product is separated from less soluble, black byproduct carbonylic species by extraction with THF and crystallized by cautiously layering 2-propanol. Yield: 0.097 g (33%). Anal. Calc for C₇₂H₄₀Ir₁₂O₂₄P₂: Ir, 63.1; C, 23.6; H, 1.1. Found: Ir, 61.9; C, 23.4; H, 1.0.

2. X-ray Analysis. Intensity Data Collection and Structure Solution and Refinement. Crystal data and other experimental details are summarized in Table I. Intensity data were collected on an Enraf-Nonius CAD-4 automated diffractometer using Mo Kα radiation (λ = 0.710 73 Å) with a graphite crystal monochromator in the incident beam. Standard CAD-4 setting, indexing, and data collection programs were used. A periodic measurement of three standard reflections revealed a crystal decay, on X-ray exposure, which was evaluated as about 15% on F₀ at the end of data collection. Lorentz, polarization, decay, and absorption corrections were applied, the last performed with the empirical method described in ref 15. The structure was determined by direct methods (MULTAN) and difference Fourier syntheses, and refinement was carried out by full-matrix least-squares procedures, the minimized function being $\sum w(F_o - k|F_c|)^2$. Individual weights were given as $w = 1/\sigma^2(F_o)$ where $\sigma(F_o) = \sigma(F_o^2)/2F_o$, $\sigma(F_o^2) = [\sigma^2(I) + (sI)^2]^{1/2}/Lp$, and s the "ignorance factor" was equal to 0.03. Anisotropic thermal parameters were assigned to iridium atoms and to the phosphorus atoms of cations while isotropic thermal parameters were assigned to all the remaining atoms. Scattering factors and anomalous dispersion corrections were taken from ref 16. The final difference Fourier map showed peaks not exceeding 0.8 e/Å³ near the metal atoms. All computations were done on a PDP 11/34 computer using the Enraf-Nonius Structure Determination Package (SDP) and the physical constants therein tabulated,[17] MULTAN[18] for direct methods, and ORTEP for drawings.[19]

(13) Osella, D.; Gambino, O.; Gobetto, R.; Zanello, P.; Laschi, F.; Housecroft, C. E.; Owen, S. M. *Organometallics* **1990**, *9*, 1792.

(14) Zanello, P.; Bartocci, C.; Maldotti, A.; Traverso, O. *Polyhedron* **1983**, *2*, 791.

(15) North, A. C. T.; Phillips, D. C.; Mathews, F. S. *Acta Crystallogr., Sect. A: Cryst. Phys. Diffr. Theor., Gen. Crystallogr.* **1968**, *A24*, 351.

(16) *International Tables for X-Ray Crystallography*; Kynoch Press: Birmingham, England, 1974; Vol. 4.

(17) B. A. Frenz and Associates. *SDP Plus Version 1.0*; Enraf-Nonius: Delft, The Netherlands, 1980.

(18) Germain, G.; Main, P.; Woolfson, M. M. MULTAN, a system of computer programs for the automatic solution of crystal structures from X-ray diffraction data. *Acta Crystallogr.* **1971**, *A27*, 368.

Results

1. Synthesis of [Ir₁₂(CO)₂₄]²⁻. In a previous paper we reported the synthesis of [Ir₆(CO)₁₅{Cu(NCMe)}]⁻.[9] This compound is unstable in refluxing THF, giving a new carbonyl compound which showed IR bands in the CO stretching region at 2020 (vs), 1990 (sh), and 1800 (m) cm⁻¹. However the latter product was not formulated owing to contradictory analytical and spectroscopic data; when the synthesis was optimized, good-quality single crystals of the tetraphenylphosphonium salt were obtained: according to elemental analysis and X-ray data, it is now possible to formulate it correctly as [PPh₄]₂[Ir₁₂(CO)₂₄]. The thermal transformation of [Ir₆(CO)₁₅{Cu(NCMe)}]⁻ into [Ir₁₂(CO)₂₄]²⁻ presumably proceeds through the intermediate formation of [Ir₁₂(CO)₂₆]²⁻; the formation of [Ir₁₂(CO)₂₆]²⁻ was proved to occur to a lesser extent at room temperature.[9] A test conducted on a microscale (refluxing MeCN) showed that [Ir₁₂(CO)₂₆]²⁻ is unstable and, after about 4 h, a greenish solution with IR bands almost coincident with those of [Ir₁₂(CO)₂₄]²⁻ is formed. The very small amount of [Ir₁₂(CO)₂₆]²⁻ available precluded the possibility of isolating the final product and identifying it unambiguously.[9]

The dianion is air-stable in the solid state for a few days; no decomposition results upon refluxing a THF or MeCN solution of [Ir₁₂(CO)₂₄]²⁻ under nitrogen for several hours. [Ir₁₂(CO)₂₄]²⁻ in THF solution is not affected by an excess of halide ions, nor does it react with acids to give a protonated derivative. The dodecanuclear complex does not react with either carbon monoxide or hydrogen (at room temperature and at atmospheric pressure) over a long period of time. In agreement with the structure found by X-ray analysis, the IR spectrum of [PPh₄]₂[Ir₁₂(CO)₂₄] shows ν_{CO} absorptions at 2067 (vw), 2021 (vs), 1989 (m), 1934 (w), 1831 (sh), and 1801 (m, br) cm⁻¹ (THF solution), attributable to terminal and edge bridging carbonyl groups.

The same anion has been observed for the first time by treating Ir₄(CO)₁₂ in 2-methoxyethanol with KOH under hydrogen. This reaction was devised to synthesize hypothetical clusters of formula [H₅₋ₓIr₁₃(CO)₂₄]ˣ⁻ (x = 1–4) and reproduces the experimental conditions employed for the preparation of the analogous rhodium clusters.[20] Small amounts of [PPh₄]₂[Ir₁₂(CO)₂₄] were actually obtained, and intense efforts have been devoted to increase the reproducibility of the reaction. Instead, we always observed the formation of mixtures of anionic carbonyl clusters, all having very similar ratios between the number of metal atoms and negative charges and, therefore, almost identical chemical and solubility properties. Some of these species have been isolated and correspond to clusters of nuclearities 9 and 10.[21] Unfortunately, this thermally induced reductive condensation had to be abandoned, since it was judged too sensitive to experimental conditions and largely less convenient than the synthesis from [Ir₆(CO)₁₅{Cu(NCMe)}]⁻, here described.

2. Molecular Structure of [PPh₄]₂[Ir₁₂(μ-CO)₅(CO)₁₉]. The crystal structure of [PPh₄]₂[Ir₁₂(CO)₂₄] consists of discrete [PPh₄]⁺ cations and [Ir₁₂(CO)₂₄]²⁻ anions packed with no short interionic contacts. The positional parameters of [PPh₄]₂[Ir₁₂-(CO)₂₄] are reported in Table II. An ORTEP view of the whole anion and the scheme used for labeling the atoms are shown in Figure 1; selected bond distances and angles are given in Tables III and IV, respectively.

The metallic frame of [Ir₁₂(CO)₂₄]²⁻ can be simply described as a ν_2 trigonal bipyramid lacking two of the vertices (one axial and one equatorial).[22] Figure 2 shows the scheme of the complete

(19) A Fortran thermal-ellipsoid program for crystal structure illustration (Johnson, C. K. *ORTEP*. Oak Ridge National Laboratory: Oak Ridge, TN, 1971).
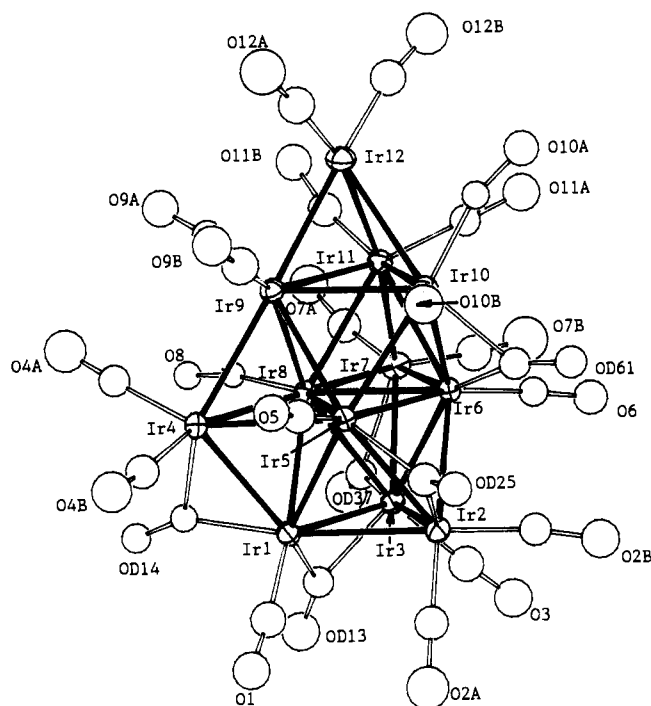
(20) (a) Albano, V. G.; Ciani, G.; Martinengo, S.; Sironi, A. *J. Chem. Soc., Dalton Trans.* **1979**, 978. (b) Albano, V. G.; Anker, W. M.; Ceriotti, A.; Chini, P.; Ciani, G.; Martinengo, S. *J. Chem. Soc., Chem. Commun.* **1975**, 1381.

(21) Della Pergola, R.; Garlaschelli, L.; Masciocchi, N.; Manassero, M. Unpublished work.

Table II. Fractional Atomic Coordinates for $[Ir_{12}(CO)_{24}]^{2-}$ Estimated (Esd's in Parentheses)

atom	x	y	z
Ir(1)	0.93785(7)	0.33804(5)	1.2722(1)
Ir(2)	0.79665(8)	0.37527(6)	1.0736(1)
Ir(3)	0.92215(7)	0.31471(5)	1.0400(1)
Ir(4)	0.86522(8)	0.25720(6)	1.3871(1)
Ir(5)	0.72087(7)	0.29343(5)	1.1919(1)
Ir(6)	0.70931(7)	0.27062(5)	0.9573(1)
Ir(7)	0.84098(8)	0.20873(6)	0.9370(1)
Ir(8)	0.83771(7)	0.23461(5)	1.1530(1)
Ir(9)	0.68255(7)	0.18528(5)	1.2202(1)
Ir(10)	0.54315(7)	0.22600(6)	1.0191(1)
Ir(11)	0.66644(7)	0.16167(5)	0.9826(1)
Ir(12)	0.52216(8)	0.11027(6)	1.0566(1)
C(1)	0.983(2)	0.404(2)	1.373(3)
C(2A)	0.861(2)	0.442(2)	1.142(3)
C(2B)	0.741(2)	0.391(2)	0.920(3)
C(3)	0.947(2)	0.367(2)	0.942(3)
C(4A)	0.906(2)	0.203(2)	1.471(3)
C(4B)	0.873(2)	0.297(2)	1.533(3)
C(5)	0.674(2)	0.304(2)	1.312(3)
C(6)	0.693(2)	0.277(1)	0.801(3)
C(7A)	0.889(2)	0.155(2)	0.960(3)
C(7B)	0.820(2)	0.202(2)	0.775(3)
C(8)	0.931(2)	0.190(1)	1.213(2)
C(9A)	0.718(2)	0.123(1)	1.262(3)
C(9B)	0.608(2)	0.186(2)	1.311(3)
C(10A)	0.418(2)	0.176(1)	0.911(3)
C(10B)	0.475(2)	0.258(1)	1.081(3)
C(11A)	0.586(2)	0.146(2)	0.823(3)
C(11B)	0.698(2)	0.102(2)	1.010(3)
C(12A)	0.450(2)	0.084(2)	1.142(3)
C(12B)	0.436(2)	0.059(2)	0.935(3)
C(D13)	1.041(2)	0.356(1)	1.193(3)
C(D14)	1.018(2)	0.300(1)	1.406(3)
C(D25)	0.680(2)	0.362(2)	1.133(3)
C(D37)	0.994(2)	0.268(2)	1.020(3)
C(D61)	0.569(2)	0.287(1)	0.906(3)
O(1)	1.009(2)	0.442(1)	1.441(2)
O(2A)	0.902(2)	0.489(1)	1.191(2)
O(2B)	0.708(2)	0.410(1)	0.825(2)
O(3)	0.962(2)	0.396(1)	0.874(2)
O(4A)	0.932(2)	0.167(1)	1.518(2)
O(4B)	0.872(2)	0.315(1)	1.612(2)
O(5)	0.642(1)	0.310(1)	1.384(2)
O(6)	0.679(1)	0.287(1)	0.699(2)
O(7A)	0.910(2)	0.108(1)	0.969(2)
O(7B)	0.795(2)	0.197(1)	0.669(3)
O(8)	0.998(1)	0.1714(9)	1.259(2)
O(9A)	0.749(2)	0.087(1)	1.303(2)
O(9B)	0.562(2)	0.182(1)	1.378(2)
O(10A)	0.339(1)	0.157(1)	0.830(2)
O(10B)	0.428(2)	0.275(1)	1.132(2)
O(11A)	0.536(2)	0.134(1)	0.714(2)
O(11B)	0.709(2)	0.052(1)	1.011(2)
O(12A)	0.404(2)	0.069(1)	1.206(3)
O(12B)	0.387(2)	0.031(1)	0.841(2)
O(D13)	1.131(2)	0.378(1)	1.221(2)
O(D14)	1.100(1)	0.2956(9)	1.466(2)
O(D25)	0.620(1)	0.387(1)	1.129(2)
O(D37)	1.077(2)	0.262(1)	1.010(2)
O(D61)	0.511(1)	0.303(1)	0.838(2)

Figure 1. ORTEP drawing and atom-labeling scheme for $[Ir_{12}(CO)_{24}]^{2-}$. Thermal ellipsoids are drawn at 30% probability. Carbonyl carbons are designated analogously to the oxygens to which they are attached.

The metal cage of $[Ir_{12}(CO)_{26}]^{2-}$ is composed by four staggered triangles in an A,B,A,B sequence, as in hexagonal close-packed lattices;[8] on the contrary, iridium bulk metal adopts a face-centered-cubic lattice.

The metal skeleton of $[Ir_{12}(CO)_{24}]^{2-}$ generates a rather irregular metal surface and, notably, a triangular face composed of six iridium atoms [Ir(4), Ir(7), Ir(8), Ir(9), Ir(11), and Ir(12)], which is, up to now, the largest flat surface known in iridium clusters. The idealized symmetry of the metal skeleton is C_s, with the mirror plane including the Ir(2), Ir(8), Ir(10), and Ir(12) atoms; however, taking also the carbonyl distribution into consideration, the mirror plane is lost and the whole anion has no symmetry elements.

The Ir–Ir bond distances are scattered in the range 2.654-(1)–2.939(1) Å, with an average value of 2.768 Å. No significant differences can be noticed between the interlayer (average 2.757 Å) and the intralayer (average 2.770 Å) distances. However, within the layers a close relationship can be observed between the metal connectivity and the average metal–metal distances; thus (i) the layer formed by atoms Ir(1), Ir(2), and Ir(3), with the lowest metal connectivity, shows the longest average distance (2.84 Å), (ii) the layer composed of Ir(4), Ir(5), Ir(6), Ir(7), and Ir(8) atoms, with the highest metal connectivity, shows the shortest average separation (2.74 Å), and (iii) the layer including atoms Ir(9), Ir(10), and Ir(11) has an intermediate average metal–metal bond length of 2.79 Å. Finally, a peculiar situation is found for the apical Ir(12) atom. On considering that the Ir-(10)–Ir(12) distance is quite long (2.939 Å) and indicative of a weak interaction, it is reasonable to describe the Ir(12) atom with an almost square planar coordination; the maximum deviation from the best plane of atoms Ir(9), Ir(11), Ir(12), C(12A), and C(12B) is ±0.08 Å, with the two terminal carbon monoxide groups *trans* to the two very short metal–metal bonds [Ir(11)–Ir(12) = 2.656 Å, Ir(9)–Ir(12) = 2.672 Å], which are the shortest metal–metal interactions found in the whole anion. Nineteen out of the twenty-four carbonyls are terminal, and the remaining five are edge-bridging. The average bond lengths Ir–$C_{terminal}$ (1.82 Å), Ir–$C_{bridging}$ (2.05 Å), C–$O_{terminal}$ (1.19 Å), and C–$O_{bridging}$ (1.19

ν_2 bipyramid, and the metal core of $[Ir_{12}(CO)_{24}]^{2-}$ is evidenced by the solid lines. This close-packed arrangement consists of a stack of four layers formed by 1, 3, 5, and 3 iridium atoms, alternating in an A,B,C,B sequence. The disposition of the metal atoms in $[Ir_{12}(CO)_{24}]^{2-}$ is an example of a mixed cubic and hexagonal close-packing; the alternate sequence of metal atoms found in $[Ir_{12}(CO)_{24}]^{2-}$ is present in several binary phases[23] and in some of the lanthanides[23] but rarely in metal clusters; known examples are $[Rh_{22}(CO)_{37}]^{4-}$ [24] and $[Os_{17}(CO)_{36}]^{2-}$.[25]

(22) Teo, B. K.; Sloane, N. J. A. *Inorg. Chem.* **1985**, *24*, 4545.
(23) Wells, A. F. In *Structural Inorganic Chemistry*, 5th ed.; Clarendon Press: Oxford, England, 1987.
(24) Martinengo, S.; Ciani, G.; Sironi, A. *J. Am. Chem. Soc.* **1980**, *102*, 7564.

(25) Charalambous, E.; Gade, L. H.; Johnson, B. F. G.; Lewis, J.; McPartlin, M.; Powell, H. R. *J. Chem. Soc., Chem. Commun.* **1990**, 688.

Table III. Interatomic Distances (Å) in $[Ir_{12}(CO)_{24}]^{2-}$ (Esd's in Parentheses)

| Ir–Ir			
Ir(1)–Ir(2)	2.825(1)	Ir(5)–Ir(9)	2.719(1)
Ir(1)–Ir(3)	2.749(1)	Ir(5)–Ir(10)	2.746(1)
Ir(1)–Ir(4)	2.708(1)	Ir(6)–Ir(7)	2.846(1)
Ir(1)–Ir(5)	2.845(1)	Ir(6)–Ir(8)	2.701(1)
Ir(1)–Ir(8)	2.744(1)	Ir(6)–Ir(10)	2.788(1)
Ir(2)–Ir(3)	2.805(1)	Ir(6)–Ir(11)	2.731(1)
Ir(2)–Ir(5)	2.771(1)	Ir(7)–Ir(8)	2.687(1)
Ir(2)–Ir(6)	2.747(1)	Ir(7)–Ir(11)	2.796(1)
Ir(3)–Ir(6)	2.788(1)	Ir(8)–Ir(9)	2.718(1)
Ir(3)–Ir(7)	2.727(1)	Ir(8)–Ir(11)	2.748(1)
Ir(3)–Ir(8)	2.755(1)	Ir(9)–Ir(10)	2.876(1)
Ir(4)–Ir(5)	2.812(1)	Ir(9)–Ir(11)	2.811(1)
Ir(4)–Ir(8)	2.710(1)	Ir(9)–Ir(12)	2.672(1)
Ir(4)–Ir(9)	2.802(1)	Ir(10)–Ir(11)	2.860(1)
Ir(5)–Ir(6)	2.796(1)	Ir(10)–Ir(12)	2.939(1)
Ir(5)–Ir(8)	2.692(1)	Ir(11)–Ir(12)	2.654(1)

Ir–$C_{terminal}$			
Ir(1)–C(1)	1.86(3)	Ir(8)–C(8)	1.91(2)
Ir(2)–C(2A)	1.75(3)	Ir(9)–C(9A)	1.81(3)
Ir(2)–C(2B)	1.79(3)	Ir(9)–C(9B)	1.82(3)
Ir(3)–C(3)	1.84(3)	Ir(10)–C(10A)	1.90(2)
Ir(4)–C(4A)	1.79(3)	Ir(10)–C(10B)	1.78(2)
Ir(4)–C(4B)	1.95(3)	Ir(11)–C(11A)	1.79(2)
Ir(5)–C(5)	1.87(3)	Ir(11)–C(11B)	1.79(3)
Ir(6)–C(6)	1.81(2)	Ir(12)–C(12A)	1.76(3)
Ir(7)–C(7A)	1.66(2)	Ir(12)–C(12B)	1.78(3)
Ir(7)–C(7B)	1.85(3)		

C–$O_{terminal}$			
C(1)–O(1)	1.15(3)	C(8)–O(8)	1.14(2)
C(2A)–O(2A)	1.22(3)	C(9A)–O(9A)	1.13(3)
C(2B)–O(2B)	1.20(3)	C(9B)–O(9B)	1.22(3)
C(3)–O(3)	1.15(3)	C(10A)–O(10A)	1.17(2)
C(4A)–O(4A)	1.14(3)	C(10B)–O(10B)	1.23(2)
C(4B)–O(4B)	1.06(3)	C(11A)–O(11A)	1.22(3)
C(5)–O(5)	1.14(3)	C(11B)–O(11B)	1.30(3)
C(6)–O(6)	1.19(2)	C(12A)–O(12A)	1.21(3)
C(7A)–O(7A)	1.30(3)	C(12B)–O(12B)	1.19(4)
C(7B)–O(7B)	1.16(3)		

Ir–$C_{bridging}$			
Ir(1)–C(D13)	2.04(2)	Ir(4)–C(D14)	2.15(2)
Ir(1)–C(D14)	1.99(2)	Ir(5)–C(D25)	2.02(3)
Ir(2)–C(D25)	2.05(2)	Ir(6)–C(D61)	2.05(2)
Ir(3)–C(D13)	2.02(2)	Ir(7)–C(D37)	2.21(2)
Ir(3)–C(D37)	1.84(2)	Ir(10)–C(D61)	2.13(3)

C–$O_{bridging}$			
C(D13)–O(D13)	1.20(2)	C(D37)–O(D37)	1.31(3)
C(D14)–O(D14)	1.17(2)	C(D61)–O(D61)	1.09(2)
C(D25)–O(D25)	1.19(3)		

Table IV. Angles (deg) in $[Ir_{12}(CO)_{24}]^{2-}$ (Esd's in Parentheses)

Ir–C–$O_{terminal}$			
Ir(1)–C(1)–O(1)	175(3)	Ir(8)–C(8)–O(8)	169(2)
Ir(2)–C(2A)–O(2A)	177(2)	Ir(9)–C(9A)–O(9A)	171(2)
Ir(2)–C(2B)–O(2B)	170(2)	Ir(9)–C(9B)–O(9B)	174(3)
Ir(3)–C(3)–O(3)	174(3)	Ir(10)–C(10A)–O(10A)	163(2)
Ir(4)–C(4A)–O(4A)	176(3)	Ir(10)–C(10B)–O(10B)	173(2)
Ir(4)–C(4B)–O(4B)	175(3)	Ir(11)–C(11A)–O(11A)	176(2)
Ir(5)–C(5)–O(5)	178(3)	Ir(11)–O(11B)–O(11B)	169(2)
Ir(6)–C(6)–O(6)	173(2)	Ir(12)–C(12A)–O(12A)	176(2)
Ir(7)–C(7A)–O(7A)	170(2)	Ir(12)–O(12B)–C(12B)	167(2)
Ir(7)–C(7B)–O(7B)	172(3)		

Ir–$C_{bridging}$–Ir			
Ir(1)–C(D13)–Ir(3)	85(1)	Ir(3)–C(D37)–Ir(7)	84(1)
Ir(1)–C(D14)–Ir(4)	82(1)	Ir(6)–C(D61)–Ir(10)	84(1)
Ir(2)–C(D25)–Ir(5)	86(1)		

Ir–C–$O_{bridging}$			
Ir(1)–C(D13)–O(D13)	139(2)	Ir(5)–C(D25)–O(D25)	142(2)
Ir(3)–C(D13)–O(D13)	136(2)	Ir(3)–C(D37)–O(D37)	148(2)
Ir(1)–C(D14)–O(D14)	145(2)	Ir(7)–C(D37)–O(D37)	125(2)
Ir(4)–C(D14)–O(D14)	133(2)	Ir(6)–C(D61)–O(D61)	147(2)
Ir(2)–C(D25)–O(D25)	132(2)	Ir(10)–C(D61)–O(D61)	126(2)

Å) are comparable with those found in other anionic iridium carbonyl clusters.[4–9]

3. Electrochemistry. Figure 3a shows the redox propensity of
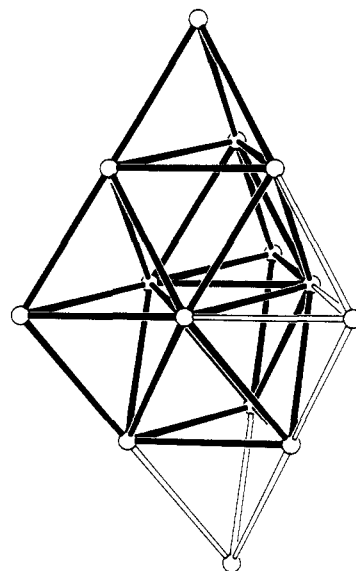
Figure 2. Schematic representation of the ν_2 bipyramid. The Ir_{12} metal core is represented by solid lines.

$[Ir_{12}(CO)_{24}]^{2-}$ in acetonitrile solution. It undergoes two reduction as well as two oxidation processes at peaks A, B and C, D, respectively. Controlled-potential coulometric tests show that both the first catodic step ($E_w = -1.1$ V) and the first anodic step ($E_w = +0.4$ V) consume two electrons per molecule. Since all the redox changes exhibit similar peak heights, we confidently assume that all the remaining electron transfers also involve two-electron exchanges, at least on the time scale of cyclic voltammetry.

As illustrated in Figure 3c for peak system C/C', the backward-to-forward peak current ratios relevant to the redox steps occurring at peaks B, C, D are always lower than unity at low scan rates. This indicates that the corresponding primarily electrogenerated two-electron congeners are only transient.[26] On the other hand, the presence of minor back-responses such as E, F, G precludes to their slow irreversible decomposition. As matter of fact, after one cycle of exaustive two-electron oxidation at peak C ($E_w = +0.4$ V) followed by exaustive reduction at peak C' ($E_w = 0.0$ V), the dianion is recovered in about 50% of the starting amount.

The reduction process occurring at peak A, which displays the associated reoxidation at peak H, proved to be more interesting (Figure 3b). After exhaustive two-electron addition ($E_w = -1.1$ V), the voltammetric pattern appears simply reversed; i.e., the two-electron-reduced species oxidizes at peak H, manifesting the reduction peak A in the reverse scan. The further coulometric reoxidation ($E_w = -0.2$ V) consumes two electrons per molecule and restores the starting cyclic voltammetric profile. This datum demonstrates that the redox change $[Ir_{12}(CO)_{24}]^{2-}/[Ir_{12}(CO)_{24}]^{4-}$ is chemically reversible, although largely departing from the electrochemical reversibility (which foresees a peak-to-peak separation of 29 mV if the second electron addition is more favoured than the first one or a peak-to-peak separation of 59 mV if the two electrons enter two noncommunicating sites).[26] Provided that unlikely redox-induced fragmentation/reaggregation processes are responsible for the chemical reversibility, such a situation is strongly reminiscent of the voltammetric behavior associated with the two-electron reduction $Os_6(CO)_{18}/[Os_6(CO)_{18}]^{2-}$, where, as pointed out by Geiger in his pioneering paper,[27] the large peak-to-peak separation is related to the large stereodynamic strain accompanying the conversion from bicapped-tetrahedral to octahedral geometry.

We schematize the overall redox aptitude of the dianion $[Ir_{12}(CO)_{24}]^{2-}$ as reported in Figure 4.

(26) Brown, E. R., Sandifer, J. R. In *Physical Methods of Chemistry. Electrochemical Methods*; Rossiter, B. W., Hamilton, J. F., Eds.; Wiley: New York, 1986; Vol. 2, Chapter 4.
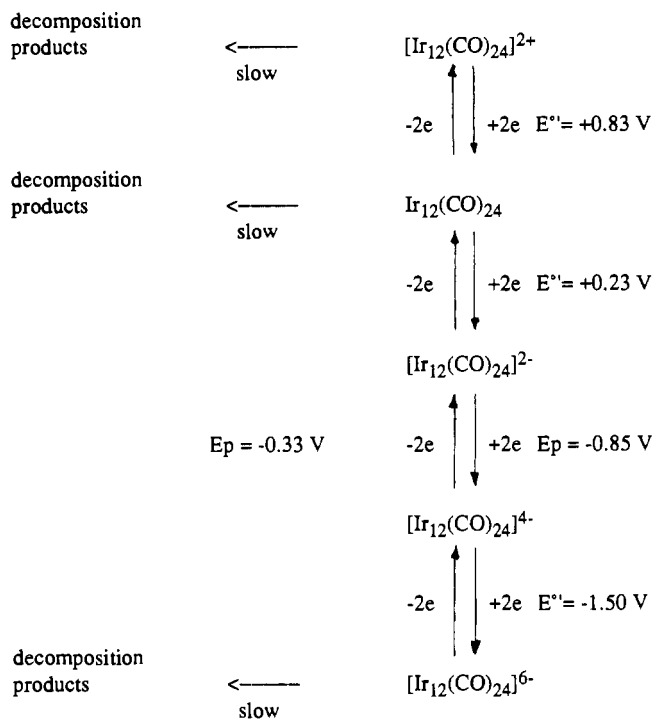
(27) Tulyathan, B.; Geiger, W. E. *J. Am. Chem. Soc.* **1985**, *107*, 5960.
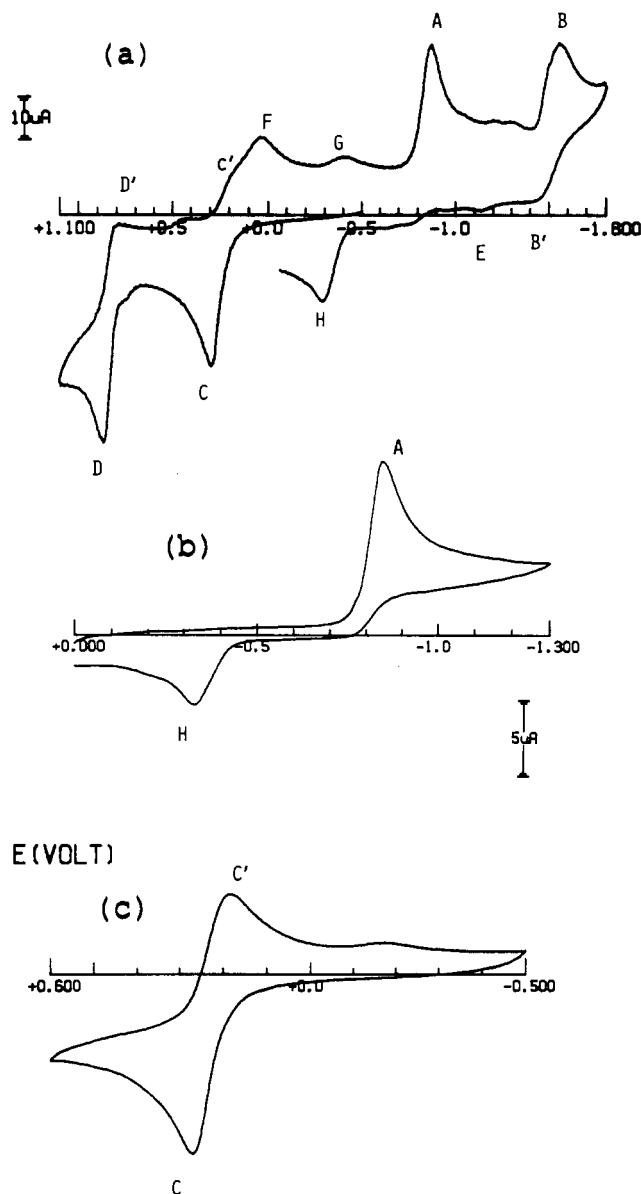
Figure 3. Cyclic voltammetric responses recorded at a platinum electrode on a deaerated MeCN solution containing [PPh$_4$]$_2$[Ir$_{12}$(CO)$_{24}$] (1.0 × 10^{-3} mol dm^{-3}) and [NEt$_4$]ClO$_4$ (0.2 mol dm^{-3}). Scan rates: (a) 0.2 V s^{-1}; (b, c) 0.02 V s^{-1}.

Figure 4. Scheme of the redox aptitude of [Ir$_{12}$(CO)$_{24}$]$^{2-}$.

Discussion

The [Ir$_{12}$(CO)$_{24}$]$^{2-}$ cluster processes 158 cluster valence electrons (CVE), corresponding to 79 cluster valence molecular orbitals (CVMO).[28] Ciani and Sironi[29] have calculated the number of filled orbitals in bare clusters formed by arrays of close-packed atoms; most of them, especially those which have very high metal to metal connectivities, conform to the $6N + 7$ rule, where N is the number of metal atoms; however, for the framework of [Ir$_{12}$(CO)$_{24}$]$^{2-}$, a value of 80 CVMO ($6N + 8$) was computed.[29] The observed value of 79 CVMO can be rationalized considering the 16-electron configuration of the square-planar Ir(12) atom (*vide supra*). Envisaging the metal skeleton of [Ir$_{12}$(CO)$_{24}$]$^{2-}$ as formed by a face-sharing bioctahedron, fused to two trigonal bipyramids through two butterflies and further capped on a triangular face, the polyhedral skeletal electron pair approach would have predicted [86 × 2 − 48 − 2(72 − 62) + 12] = 156 CVE.[30] The same value can be found according to the topological electron counting scheme ($8V - F + X + 2 = 78$

CVMO), with 12 vertices, 20 faces, and $X = 0$, for two octahedra and two hidden edges.[31]

Strict similarities can be found with the metal skeleton of the recently reported [Ru$_{11}$H(CO)$_{27}$]$^{3-}$,[32] which can be derived by the ν_2 trigonal bipyramid by removing one equatorial and both apical vertices. The numbers of CVE observed in [HRu$_{11}$-(CO)$_{27}$]$^{3-}$ (146) and in [Ir$_{12}$(CO)$_{24}$]$^{2-}$ are related by the capping principle.[2f,30]

Other carbonyl cluster with a truncated ν_2 bipyramidal metal geometry are known in the literature: e.g. [Ni$_{12}$(CO)$_{21}$H$_{4-n}$]$^{n-}$ (n = 2–4)[33] and the structurally related mixed-metal carbonyl clusters [Ni$_9$Pt$_3$(CO)$_{21}$H$_{4-n}$]$^{n-}$ (n = 2–4).[34] However, two major differences can be pointed out in the latter compounds: (i) they possess 166 CVE, 8 more than [Ir$_{12}$(CO)$_{24}$]$^{2-}$ (this discrepancy is probably related to the presence of long interlayer metal–metal bonds[31]), and (ii) both missing vertices are in the apical position and the resulting metal frames possess a D_{3h} symmetry.

The unprecedented metal cage of [Ir$_{12}$(CO)$_{24}$]$^{2-}$ is determined by electronic and steric requirements, rather than geometrical arguments: the present compound adopts a metal core of low symmetry, with irregular surfaces, in order to accommodate the large number of ligands required to saturate its skeletal orbitals. In spite of its shape, and its anomalous electron counting, the cluster exhibits a rather elevated stability. The correspondence between the structure adopted and the electron requirements is witnessed by the electrochemical studies, since the addition of two electrons induces severe structural modifications.

Supplementary Material Available: Full lists of crystallographic data, positional parameters, anisotropic and isotropic thermal parameters, and bond distances and angles (17 pages). Ordering information is given on any current masthead page.

(28) (a) Lauher, J. W. *J. Am. Chem. Soc.* **1978**, *100*, 5306. (b) *Ibid.* **1979**, *101*, 2604.
(29) Ciani, G.; Sironi, A. *J. Organomet. Chem.* **1980**, *197*, 233.

(30) Mingos, D. M. P. *Acc. Chem. Res.* **1984**, *17*, 311.
(31) Teo, B. K.; Longoni, G.; Chung, F. R. K. *Inorg. Chem.* **1984**, *23*, 1257.
(32) Bailey, P. J.; Beswick, M. A.; Johnson, B. F. G.; Lewis, J.; Raithby, P. R.; Ramirez de Arellano, M. C. *J. Chem. Soc., Dalton Trans.* **1992**, 3159.
(33) (a) Broach, R. W.; Dahl, L. F.; Longoni, G.; Chini, P.; Schultz, A. J.; Williams, J. M. *Adv. Chem. Ser.* **1978**, *167*, 93. (b) Ceriotti, A.; Chini, P.; Della Pergola, R.; Longoni, G. *Inorg. Chem.* **1983**, *22*, 1595.
(34) Ceriotti, A.; Demartin, F.; Longoni, G.; Manassero, M.; Piva, G.; Piro, G.; Sansoni, M.; Heaton, B. T. *J. Organomet. Chem.* **1986**, *301*, C5.